Numerical Simulation of Performance Improvement of Underwater Lidar by Using a Spiral Phase Plate as Spatial Filter

YingQi Liao, SuHui Yang, Kun Li, Yan Hao, Zhuo Li, Xin Wang, and JinYing Zhang

***Abstract*—In turbid water, target reflected lidar signal is easily buried in "clutter" due to scattering. We proposed an underwater laser ranging model applying an optical vortex in the receiver to separate the scattering clutter from the target reflected signal. A spiral phase plate (SPP) was placed in front of the detector to convert the target reflected Gaussian beam to an optical vortex. While the scattering clutters were not able to be converted due to the loss of spatial coherence. Therefore, the target reflected signal and scattering clutters were spatially separated by the SPP. An underwater laser detection simulation using Zemax software was carried out. The numerical simulation showed that when the SPP was placed in front of the receiver, the contrast of signal to clutter of the detection was improved by blocking the scattering clutters which had a Gaussian distribution at the center on the detection plane. The effects of beam divergence and orbital angular momentum (OAM) order to the lidar performance were also analyzed.**

***Index Terms*—Scattering, imaging systems, mie theory.**

I. Introduction

WHEN a light beam travels in water, it experiences absorption and scattering. Duntley and his coworkers found that the attenuation of light from 0.47∼0.58 um wavelength in seawater was much smaller than other wavelengths [1], as if there was a blue-green window in the ocean where light can go through. This fact makes underwater lidar and light communication possible. By using green and blue light as the light source in seawater, the absorption loss can be greatly reduced. However, scattering remains a big challenge for underwater lidar. Scattering causes spatial and temporal dispersion of the target reflected signal. Spatial dispersion refers to the light reaching the detector with a wider angle due to photons collide with particles in the water. Temporal dispersion refers to the extension of time that photons reach the detector. This is because of the different propagating paths of the ballistic photons and the multiple scattered photons.

Manuscript received September 24, 2021; revised October 24, 2021; accepted November 1, 2021. Date of publication November 4, 2021; date of current version November 16, 2021. This work was supported in part by the National Natural Science Foundation of China under Grants 61835001 and 61875011, and in part by the China Postdoctoral Science Foundation under Grant 2020TQ0036. *(Corresponding author: SuHui Yang.)*

The authors are with the Department of School of Optics and Photonics, Beijing Institute of Technology, Beijing 100081, China (e-mail: 1837936162@qq.com; suhuiyang@bit.edu.cn; likun0377@126.com; bithaoyan@163.com; lizhuo@bit.edu.cn; wangxin@bit.edu.cn; jyzhang@bit.edu.cn).

Digital Object Identifier 10.1109/JPHOT.2021.3125225

Therefore, scattering has to be overcome in underwater lidar applications. Backscatter can be suppressed by setting a time gate at the receiver [2–4], especially for the detection of long-range targets, the time gating method is very effective [5]. Intensity modulation of the detecting laser beam can also suppress backscattering light when the modulation frequency exceeds the cut-off frequency, 100 MHz in seawater, but the modulation frequency required to suppress forward scattered light is much higher [6–8]. Technologies for reducing backscatter clutter are relatively mature, but the forward scattered light often reaches the detector along with the target reflected signal and causes deterioration of underwater imaging resolution and ranging accuracy.

Recently, an optical vortex is applied in scattering-related fields [9], [10]. Optical vortex was used to separate the multiple scattering from direct transmission or target reflection due to the fact light beam with high spatial coherence can be converted onto optical vortex after passing a vortex generator, whereas multiple scattering with low spatial coherence cannot be converted onto optical vortex. Therefore, most of the photons distributed in the center of the optical vortex are scattered photons. The optical vortex was used as a window to filter out the strong probe light on the vortex to obtain weak scattering information [11]. Conversely, the application of optical vortex can also reduce the negative effects of scattering instead of detecting scattering. Blocking the strong scattering in the middle and only detect the target reflected photons on the vortex can increase the signal to clutter ratio in the underwater lidar system. Based on this hypothesis, a new method was proposed by Brandon and his coworkers, they used a spiral phase plate (SPP) in front of the receiver to distinguish the ballistic object-reflected light and scattered clutter in an underwater detection system [12]. Austin and his coworkers also used an SPP in the receiving module in an underwater ranging system and found the accuracy of ranging improved [13], in their setup, a streak camera was used to take images in clear water as well as in turbid water. The ranging accuracy improvement was achieved by subtracting the two imagines taken in clear water and turbid water. However, in a real underwater ranging application, it is not realistic to take the image of the target return in clear water as a reference. Therefore, we want to verify the effectiveness of using optical vortex to suppress forward scattering clutters by directly detecting the target return signal without taking reference and post-processing of the images.

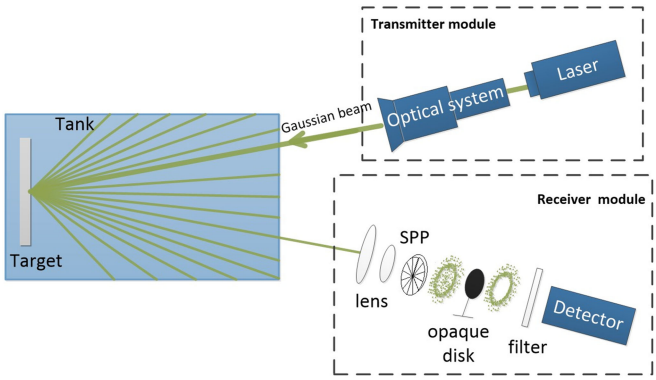

Fig. 1. An illustration showing the module of the underwater detection.

In this paper, we propose an underwater laser detection model in which an SPP is applied to separate the target reflection from forward scattering, the area within the optical vortex is blocked by an opaque plate, only the photons on the optical vortex can be detected. Based on optical design software Zemax, we simulate the signal to clutter ratio of the detection. We found that the contrast of signal to clutter of the detection can be improved by using an SPP as a spatial filter. The effects of beam divergence and OAM order to the lidar performance were also analyzed.

II. Simulation Model

A. Setup and Establishment of Light Propagation Model in Turbid Water

The underwater detection model is shown in Fig. 1. The incident Gaussian beam illuminates an object merged in water. At the receiver module, the light return from the water tank is collected with a reversely placed telescope to narrow the beamwidth before passing through an SPP. We can make the diameter of the vortex beam ring almost the same as the diameter of the detector by adjusting the lens group. The target return enters the receiving optical system contain ballistic photons, snake route photons and multiple scattered photons. Only photons with high spatial coherence can be converted to an optical vortex after passing through an SPP [14]. Multiple scattered photons lose their spatial coherence due to multiple collisions with particles in water therefore they cannot be converted to the optical vortex after passing through the SPP. While ballistic photons and part of the snake route photons which maintain their spatial coherence can be converted to the optical vortex after passing through the SPP. Photons distributed in the vortex center are mostly scattered photons which lose their spatial coherence in turbid water, carrying wrong range information. On the contrary, target reflected photons on the optical vortex carry ranging information of the detected target. If we use an opaque disk to block the area inside the optical vortex, only allow the photons on the vortex to arrive at the detector, the influence of the scattered clutter can be partly removed. Furthermore, according to the Mie scattering theory, both forward scattering and backward scattering maximize in the center. Therefore, we hope by this means, we can see improvement of the underwater lidar performance with an SPP as a spatial filter.

The collision of photons in the scattering medium is simulated by Monte Carlo method in Zemax. Zemax can trace the propagation of light and display the distribution of photons on the detection plane. We need to input the geometry and physical properties of different media that the photon encountered in the simulation. For example, we need to input the material as water then the absorption coefficient at 532 nm light is automatically given by the software. The scattering of the photon is controlled by two parameters, the scattering angle, and attenuation caused by the scattering. The scattering of photons by seawater molecules is Rayleigh scattering, compared with Mie scattering in turbid water, Rayleigh scattering can be ignored. In turbid water, Mie scattering dominants the scattering loss, so we chose the Henyey-Greenstein expression, which is commonly used to express Mie scattering in seawater, to describe the scattering in turbid seawater in the simulation model, it reads:

$$P_{HG}(\vartheta) = \frac{1-g^2}{4\pi(1+g^2-2g\cos\vartheta)^{\frac{3}{2}}} \tag{1}$$

where ϑ is scattering angle, $P_{HG}(\vartheta)$ is the probability density function with respect to angle, and $g = \langle\cos\vartheta\rangle$ is the asymmetry factor ranging from -1 to 1.

The direction of the scattered photon in the model is related to the asymmetry factor, positive value corresponds to forward scattering, and the negative value corresponds to backward scattering. In seawater, forward scattering is dominating, the value of the asymmetry factor is between 0.9 and 1 [15], so we set it as 0.95.

The attenuation caused by scattering and the attenuation caused by absorption are considered together, that is $c = a + b$, where c is total attenuation coefficient, a is absorption coefficient and b is scattering coefficient. The absorption coefficient is fixed as 0.04 m^{-1} and the scattering coefficient varies with the turbidity of the medium. The product of the attenuation coefficient c of the medium and the physical distance of the object in the medium is the attenuation length (AL), which is commonly used as a measure of underwater propagation capability in underwater lidars.

A mirror is used as the target. We also simulated objects with other surfaces, such as PVC with diffuse reflective surfaces. In this case, most of the reflected light was outside of the receiving aperture, so only a small fraction of the light within the receiving aperture can be detected as returning signals. Increasing the returning signals requires a much increase in the number of photons, which will lead to an extremely long numerical simulation time. Diffusion surface will cause more loss maybe to certain extent also reduce the coherence of the photons. But the principle of using the SPP to separate the coherent signal and incoherent multiple clutters should also apply to the diffusion surface.

The material of the lens is set to be K9 glass with a refractive index of 1.516. The opaque disk behind the SPP is set to have a light-absorbing surface, which is just big enough to cover the core of the vortex beam. The vortex beam generated by the high-order SPP has a larger center diameter, therefore, a bigger opaque

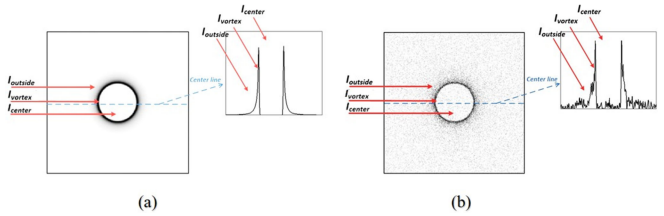

Fig. 2. The distribution of optical return in (a) clean water and (b) turbid water.

disk is needed for blocking the central area when high-order SPP is used.

B. Setting and Analysis of Optical Vortex

There are many methods for generating optical vortex. Among them, the method of using an SPP has high conversion efficiency and can be used for high-power laser beams. SPP is a transparent diffraction optical device. One surface is flat, the thickness d to the other surface increases with azimuth angle according to the following relation:

$$d(\theta) = \frac{l\lambda\theta}{2\pi(n - n_0)} \tag{2}$$

where θ is the azimuth angle, l is the order of topological charge of the SPP, λ is the wavelength in the vacuum which is 532 nm in the case, n is the index of refraction of the material which is 1.516 as we used silicon glass, n_0 is the refraction index of air which is 1. When a collimated beam is incident to the SPP, the light at different azimuth angle experience different optical path length, therefore, the phase shift is different which turned the wavefront into a spiral shape. A model of SPP is generated by CAD software according to (2), and imported into Zemax.

A laser beam of amplitude u pass through the SPP, and the amplitude of the outgoing beam can be expressed as $u' = ue^{il\theta}$. This additional phase factor of $e^{il\theta}$, which carries orbital angular momentum (OAM), and forms a spiral wavefront. In the beam center, the beam experiences destructive interference, which causes the vortex beam to form a dark center where the intensity of the light is zero.

However, there has a requirement for the spatial coherence of the beam to generate an optical vortex. Fig. 2(a) shows the optical return in clean water. Since this return remained highly spatially coherent, a clear vortex ring can be observed. In this case, we divide the light return into three areas, the core inside the vortex, the optical vortex ring and the area outside the vortex. Their light intensity is respectively expressed as:

$$I_{center} = 0; I_{vortex} = I_{target}; I_{outside} = 0 \tag{3}$$

where I_{target} is the target reflected light. Since the incident laser has high spatial coherence, the light reflected by the mirror also remains the high spatial coherence, so almost all of the optical return is converted into an optical vortex by the SPP.

Fig. 2(b) shows the optical return in turbid water. Multiple scattered light loses their spatial coherence during propagation, so they cannot be converted into an optical vortex after passing through the SPP. On the contrary, the spatial coherence of the target reflected light is not degraded during propagation so after passing the SPP, those light can be converted into an optical vortex. Mathematically:

$$\begin{aligned} I_{center} &= I_{scatter}; I_{vortex} \\ &= I_{target} + I_{scatter}; I_{outside} = I_{scatter} \end{aligned} \tag{4}$$

where $I_{scatter}$ is the scattered light, which maximized in the beam center.

III. Results

The focal lengths and positions of lens, diameter and position of the opaque disk are adjusted to make the opaque disk just block the center of the vortex, preventing scattered light distributed in the vortex center from entering the detector, but not the light on the vortex. The size of the opaque disk was determined by observing the size of the optical vortex in clear water, since all the photons are converted on the optical vortex. The result was the same as that in Fig. 2(a). Then this size of the inner circle of the optical vortex was taken as the size of the opaque disk. Lens are adjusted so that the size of the ring of the vortex is comparable to the size of the detector, reducing scattered light outside the vortex get into the detector.

We divide the photons received on the detector into ballistic photons and scattered photons. The software can distinguish ballistic photons that have not been scattered in the medium and scattered photons that have been scattered, and obtain their distributions respectively. We define the ratio of the number of ballistic photons to the number of scattered photons as the contrast of signal to clutter, and use this contrast value as an indication of the influence of the optical vortex in the detection. The number of ballistic photons and the number of scattered photons are respectively calculated as the number of the ballistic photons and the number of the scattered photons received on the detector.

Snake route photons experienced less scattering and keep their spatial coherence to a large extent. Therefore, snake route photons also contribute to the optical vortex after passing through the SPP. Due to the little scattering experienced, snake route photons will basically not cause errors in detection. On the contrary, snake route photons are valuable because they can increase the energy of photons received by the detector, which is especially important in very turbid medium. However, it is not possible to distinguish the snake route photons and the multiple scattered photons in Zemax. When we calculated the contrast of signal to clutter, we regarded ballistic photons as the signal, and all photons that had been scattered as clutter including snake route photons. But in real underwater detection, snake route photons also contribute to detect.

The photons in the optical return were divided into scattered photons and ballistic photons according to whether they collided with particles in the water or not. In order to see the effect of the optical vortex at different turbidity of the water, the Al of the water was set to 2 and 9, respectively. The result in Fig. 3(a) is obtained when the AL was set to 2. It is seen that by using SPP and the opaque disk, the number of scattered photons received by the detector was reduced. However, the number of ballistic photons at low attenuation length was much higher than that

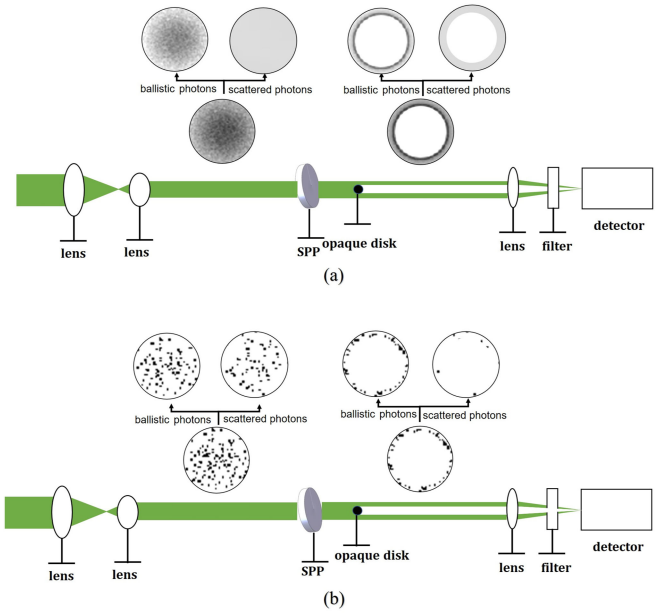

Fig. 3. The distribution of ballistic photons and scattered photons in the optical return before and after using optical vortex. (a) corresponds to AL = 2, (b) corresponds to AL = 9.

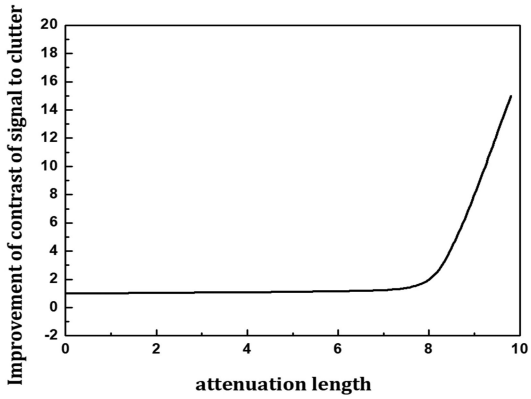

Fig. 4. The improvement of signal to clutter ratio after using optical vortex at the receiver. The improvement increases with the increase of the turbidity of the water.

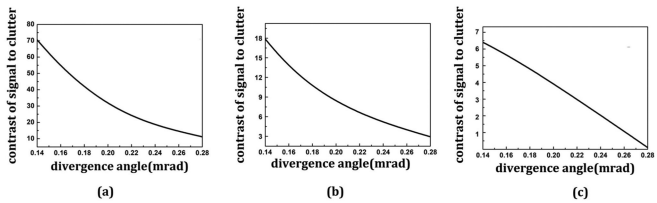

Fig. 5. The contrast of signal to clutter decreases with increase of the divergence angle of the incident light when the attenuation length is 5(a), 6(b), and 7(c).

of scattered photons, so the use of vortex light did not improve the contrast of signal to clutter very much. When AL was set to 9, the spatial distribution of photons is shown in Fig. 3(b). At large attenuation length, the number of ballistic photons and the number of scattered photons were greatly reduced so was the contrast of signal to clutter. However, with the use of optical vortex, the contrast of signal to clutter was much improved compared to not using it.

We calculated the contrast of signal to clutter with and without the use of SPP and opaque disk at different attenuation lengths. The attenuation length was changed by fixing the target position at 5 meters away from the detector and changing the turbidity of the water. The divergence angle of the incident light was 0.15 mrad, and the OAM order of the SPP in front of the detector was 16. Since the number of photons we used in the simulation was limited by the Zemax software, and the maximum number of photons was not enough to support calculations of more than 10 attenuation lengths, the received photons were too few to be analyzed. Therefore, we can only simulate to AL = 10. The improvement of contrast of signal to clutter was calculated to show the effect of the optical vortex. The improvement of contrast of signal to clutter was defined as the ratio of the contrast of signal to clutter with the use of SPP and opaque disk to the contrast of signal to clutter of the same receiving aperture without the use of SPP or opaque disk. There are also scattered photons outside the vortex. But Mie scattering shows a maximum in the center. In addition, the effective area of the detector was almost the same size as the ring of the vortex, which was achieved by controlling the optical system. Therefore, the scattering outside of the optical vortex had a negligible effect on the detection and the contrast can be improved by blocking the center of the vortex.

Fig. 4 shows the improvement of contrast of signal to clutter by using optical vortex at the receiver. Obviously, the occlusion of scattered light caused by the use of optical vortex improved the contrast of signal to clutter. The improvement is more obvious in more turbid water. In addition, there is a turning point in the improvement of contrast of signal to clutter near the attenuation length of 8. This was because although most of the target reflected signal can be converted into an optical vortex, there were some target-reflected photons remained in the center, they were snake route photons. Therefore, by blocking the center of the optical return, one blocked also part of the target reflected signal. The conversion efficiency from the target reflected signal to the optical vortex was not 100%, so there is a turning point in the improvement of the contrast of signal to clutter.

In order to analyze the effect of the divergence of the Gaussian beam on the contrast of signal to clutter of the detection, we changed the divergence angle of the Gaussian beam. The contrast of signal to clutter results with different divergence angles is shown in Fig. 5. The result was obtained when the power of the incident light source was 1 W and the OAM order of SPP was 16. One can see, the contrast decreased with the increase of the beam divergence. A larger attenuation coefficient requires a smaller divergence angle to ensure that the signal is not completely submerged by clutter. One can see that in more turbid water, in order to have the same signal-to-clutter contrast, the beam divergence needs to be even narrower.

We calculated the contrast of signal to clutter in turbid water with different orders of SPPs. The results are shown in Fig. 6, the contrast of signal to clutter increased with the increase of the order of SPP. The result was obtained when the power of the incident light source was 1 W and the divergence angle was 0.15 mrad. The reason is that the optical vortex with a large

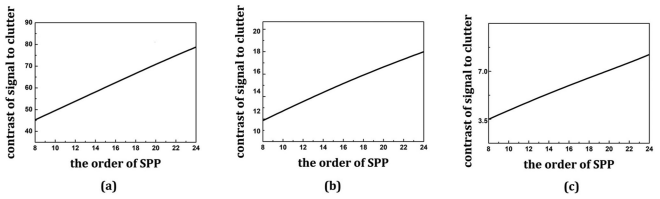

Fig. 6. The contrast of signal to clutter decreases with increase of the divergence angle of the incident light when the attenuation length is 5(a), 6(b), and 7(c).

topological charge had a larger diameter of the vortex, and the size of the opaque shelter was bigger, less scattered photons can be received in the detection area on the vortex, resulting in higher contrast. Similarly, A larger attenuation coefficient requires a higher order SPP to effectively separate the signal from clutters.

IV. Conclusion

In this paper, we propose to use an optical vortex to suppress the influence of forward scattering in underwater detection. An SPP in the receiver was used as a spatial light filter to separate the scattered light and target-reflected light based on the difference of spatial coherence between two types of optical returns. Numerical simulations show that optical vortex can improve the contrast of target reflected signal to scattering clutter in underwater detection. The influence of the beam divergence and the order of the SPP on the contrast of signal to clutter improvement were simulated and discussed. In turbid water, a higher-order SPP is more helpful to separate the scattering from the target reflected signal spatially.

The simulation results of this study provide references for underwater laser detection with an optical vortex. Corresponding experiments will be carried out to verify our theoretical predictions.

References

[1] S. Q. Duntley, "Light in the sea," *J. Opt. Soc. Amer.*, vol. 53, no. 2, pp. 214–233, 1963.

[2] G. R. Fournier, D. Bonnier, J. L. Forand, and P. W. Pace, "Range-gated underwater laser imaging system," *Opt. Eng.*, vol. 32, no. 9, pp. 2185–2190, 1993.

[3] M. E. Zevallos, S. K. Gayen, M. Alrubaiee, and R. R. Alfano, "Time-gated backscattered ballistic light imaging of objects in turbid water," *Appl. Phys. Lett.*, vol. 86, no. 1, pp. 011115-1–011115-3, 2004.

[4] D. J. Hall, J. Hebden, and D. T. Delpy, "Imaging very-low-contrast objects in breastlike scattering media with a time-resolved method," *Appl. Opt.*, vol. 36, no. 28, pp. 7270–7276, 1997.

[5] G. D. Gilbert, "High-resolution 3D underwater imaging," in *Proc. SPIE - Int. Soc. Opt. Eng.*, Denver, CO, USA, 1999, vol. 3761, pp. 10–19.

[6] F. Pellen, X. Intes, P. Olivard, Y. Guern, J. Cariou, and J. Lotrian, "Determination of sea-water cut-off frequency by backscattering transfer function measurement," *J. Phys. D: Appl. Phys*, vol. 33, pp. 349–354, 2000.

[7] L. J. JMullen and V. M. Contarino, "Hybrid LIDAR-radar: Seeing through the scatter," *IEEE Microw. Mag.*, vol. 1, no. 3, pp. 42–48, Sep. 2000.

[8] A. Laux, L. Mullen, and P. Perez, "Underwater laser range finder," in *Proc. SPIE Defense, Secur., Sens.*, Baltimore, MD, USA, 2002, vol. 8372, Art. no. 83721B.

[9] C. Brandon, M. Kaitlyn, M. Keith, J. Eric, D. Kaitlin, and M Linda. "Propagation of modulated optical beams carrying orbital angular momentum in turbid water," *Appl. Opt.*, vol. 55, no. 31, pp. C34–C38, 2016.

[10] W. B. Wang, R. Gozali, L. Shi, L. Lindwasser, and R. R. Alfano, "Deep transmission of Laguerre–Gaussian vortex beams through turbid scattering media," *Opt. Lett.*, vol. 41, no. 9, pp. 2069–2072, 2016.

[11] D. Palacios, D. Rozas, and G. A. Swartzlander, "Observed scattering into a dark optical vortex core," *Phys. Rev. Lett.*, vol. 88, no. 10, 2002, Art. no. 103902.

[12] B. Cochenour, L. Rodgers, A. Laux, L. Mullen, and E. G. Johnson, "The detection of objects in a turbid underwater medium using orbital angular momentum (OAM)," in *Proc. SPIE Defense + Secur.*, Anaheim, CA, USA, 2017, vol. 10186, Art. no. 1018603.

[13] A. Jantzi, L. Mullen, J. William, and C. Brandon., "Enhanced underwater ranging using an optical vortex," *Opt. Exp.*, vol. 26, no. 3, pp. 2668–2674, 2018.

[14] D. M. Palacios, I. D. Maleev, A. S. Marathay, and G. A. Swartzlander, "Spatial correlation singularity of a vortex field," *Phys. Rev. Lett.*, vol. 92, no. 14, 2004, Art. no. 143905.

[15] H. Xin and Z. Xiangjin. "Lasers' underwater transmission simulations in various channel environments," *J. Ordnance Equip. Eng.*, vol. 12, pp. 140–144, 2016.